Geomorphology 496 (2026) 110159

Contents lists available at ScienceDirect

Geomorphology

journal homepage: www.journals.elsevier.com/geomorphology

Field measurements of *Phragmites australis* root reinforcement and traits along a riparian zone

Abhijith Kamath[a,*], Jan-willem van de Kuilen[a,b]

[a] Department of Engineering Structures, Biobased Structures and Materials Group, Delft University of Technology, Stevinweg 1, 2628 CN, Delft, the Netherlands
[b] Wood Technology, Technical University of Munich, Winzererstrasse 45, 80797, Munich, Germany

ARTICLE INFO

Keywords:
Common reed
Root reinforcement
Bank stability
Phragmites australis

ABSTRACT

Phragmites australis L., a widespread vegetation in riparian zones such as rivers and canals, is extensively studied for its ecological benefits such as nutrient removal and hydraulic retention. However, its direct contribution to bank stability through root reinforcement, a key factor for its use in soil bioengineering techniques, has received limited attention. This study investigated the root reinforcement provided by *P. australis* and its root traits at a soil bioengineering test site on a canal bank in the Province of North-Holland in the Netherlands.

Direct measurements of root-soil composite strength were performed using a corkscrew extraction technique at two distinct distances from the canal. Concurrently, root distribution parameters, including Root Area Ratio (RAR) and Root Length Density (RLD), were quantified from extracted soil plugs. Root reinforcement was also indirectly estimated using biomechanical models, incorporating measured root tensile strength and root distribution parameters as inputs. A total of 12 excavations, each 0.25 m^2, were conducted for comprehensive root trait analysis at both locations.

Direct measurements revealed substantial root reinforcement (max 36 kPa; avg 6–19 kPa). RAR showed effective stabilization values between 0.03 and 0.65 %, peaking at 0.65 % in the area close to canal. Root systems were dominated by fine roots (<0.5 mm diameter), comprising >80 % of total root length and creating dense reinforcing networks. Corkscrew measurements yielded conservative values. Modeled estimates significantly exceeded these field measurements, which is consistent with conventional shear testing. The extensive root surface area (>3.9 $m^2\ m^{-2}$) further demonstrates the species' soil-binding capacity, with higher values occurring in hydrologically favorable zones.

While the ecological implications of using this widespread species must be contextually considered, its pronounced mechanical reinforcement makes it a highly effective biotechnical tool, particularly in managed environments like canals.

1. Introduction

Phragmites australis L. (P.australis) commonly known as common reed is a prevalent vegetation along rivers and canal banks in many parts of the world. *P.australis* is a highly resilient species, found across a vast array of global ecosystems, from saturated wetlands like saltmarshes, fens, and lake edges to drier terrestrial sites where competitor pressure is minimal (Haslam, 1970; Romero et al., 1999).

P.australis have demonstrated high tolerance for waterlogging and low-oxygen conditions (Haslam, 1972; Pagter et al., 2005). The superior performance of *P.australis* in nutrient-rich (eutrophic) environments with high nitrogen and phosphorus availability is also well-documented, a trait supported by its capacity for significant biomass production, effective nutrient removal, and its utility in environmental phosphorus control (Uddin and Robinson, 2018; Geurts et al., 2020; Carricondo et al., 2021). Beyond its nutrient roles, *P.australis* has demonstrated potential for phytoremediation, notably in the effective removal of polyfluoroalkyl substances pollutants from contaminated water (Ferrario et al., 2022). Therefore, *P.australis* is also a plant of choice for constructed wetlands, ecological restoration of wetlands and in riparian buffer zones (Uchida and Tazaki, 2005; Wang et al., 2012; Moulisova et al., 2023; Li et al., 2024).

However, the management of *P.australis* requires a balanced perspective, as its vigorous growth can present ecological challenges. *P.*

* Corresponding author.
E-mail address: A.C.Kamath@tudelft.nl (A. Kamath).

https://doi.org/10.1016/j.geomorph.2026.110159
Received 1 August 2025; Received in revised form 1 January 2026; Accepted 2 January 2026
Available online 7 January 2026

australis is a fundamental native component of wetland and riparian ecosystems across Europe. Nevertheless, its robust clonal expansion may lead to the formation of dense monodominant stands that alter habitat structure and reduce native plant diversity (Rudrappa et al., 2009; Vila et al., 2011). This is consistent with global patterns where dominant plant species, even native ones, can significantly impact local communities. Furthermore, such dominance can disrupt natural plant successions (Fogliata et al., 2021). Therefore, a comprehensive understanding of *P.australis*—encompassing both its functional benefits and its potential ecological impacts—is crucial for sustainable riparian zone management.

Even though widely spread along river and canal banks, its direct contribution to bank stability through root reinforcement, a key factor for its use in soil bioengineering techniques (Rey et al., 2019), has received limited attention. In general, riparian vegetation has shown to improve the stability of stream banks through hydro-mechanical reinforcement at the rooted zone (Simon and Collison, 2002; Pollen and Simon, 2005; Andreoli et al., 2020). Mechanical reinforcement due to roots, root reinforcement, is generally represented by an increased cohesion term and included in bank stability models (Capobianco et al., 2021). Riparian root reinforcement is either measured directly using field shear strength measurements (Zhang et al., 2018) or indirectly using models developed to estimate the shear strength increase due to the root reinforcement (Andreoli et al., 2020). The interpretive models utilize the quantity of roots obtained from root sampling as well as strength of roots (Waldron, 1977; Pollen and Simon, 2005). Root tensile strength is dependent on the diameter of the roots and generally a power law relationship is seen to fit the best between root diameter and the strength (e.g. Boldrin et al., 2021; Meijer, 2024).

Krzeminska et al. (2019) suggested that for gentle slope grass root reinforcement might provide sufficient reinforcement, while for steeper slopes trees provide the best reinforcement. However, in cohesive material, the self-weight of the trees could contribute to the instability and could be decisive where the bank itself is inherently unstable (Abernethy and Rutherfurd, 2000; Török and Parker, 2022). Direct field measurements of root reinforcement from common canal bank vegetation like *P. australis* are rarely reported in the literature. Based on root sampling, Yu et al. (2020) showed that additional root reinforcement due to *P.australis* enhanced riverbank stability by 88.2 % compared to non-vegetated conditions. Li et al. (2024) conducted laboratory direct shear tests on undisturbed *P.australis* root-soil composite under a normal stress range of 25–200 kPa and observed an increase in shear strength primarily due to an increase in cohesion of 9.97–18.69 kPa of the composite compared to bare soil.

Traditional approaches to quantifying *P.australis* root reinforcement, often involving laboratory testing of prototypically sampled root-soil composites or laborious direct root sampling, present significant challenges for large-scale catchment field testing (Meijer et al., 2018). This study addresses these methodological constraints by applying the corkscrew extraction technique (Meijer, 2016; Meijer et al., 2018; Meijer et al., 2019) for direct, in-situ assessment of root reinforcement—to *P.australis*-vegetated canal banks at two distinct distances from the water source to obtain a general spread of potential root reinforcement. The research further complements these direct measurements with estimations from interpretive models and detailed characterization of root structural traits derived from excavated monoliths.

2. Materials and methods

2.1. Site conditions

The study was conducted along a canal bank located near to Middenmeer, Provincie Noord-Holland, The Netherlands (Fig. 1 (a)). The canal was protected by a hardwood (*Azobe*) timber sheet pile. Behind the sheet pile was a flat region of about 2 m and followed by a slope of 1 vertical to 3 horizontal.

The soil at the study site was classified as poorly graded sand under the USCS classification (See supplementary material S1). Fine sand with seashells was observed at depth below 0.5 m. In October 2022, rhizomes of *P.australis*, was planted in a 10 by 5 m area behind the sheet pile (Fig. 1 (b)). The planting density was 25 rhizomes per m^2. The study area was left undisturbed for a period of 20 months Fig. 2.

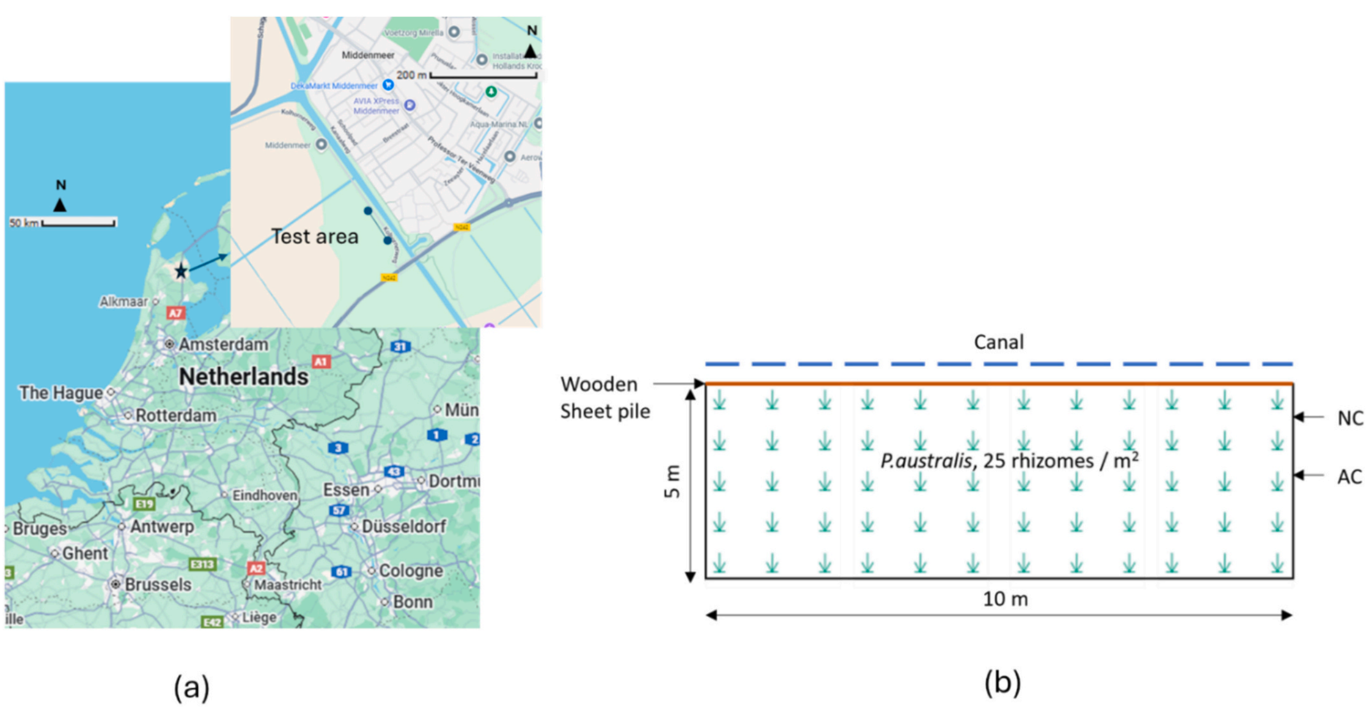

Fig. 1. (a) Test area on the map (b) Schematic drawing of planting and the test locations NC-Near canal and AC-Away from the canal.

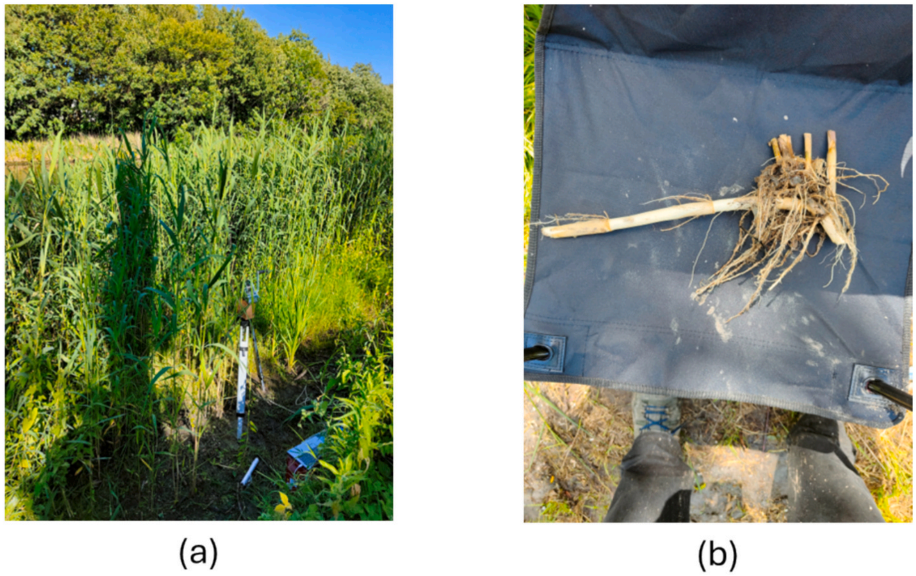

Fig. 2. (a) *P.australis* growth and test setup at test site (b) an example of below ground rhizome and root system excavated from the site.

2.2. Soil strength measurement

The strength of both unrooted soil and root-reinforced soil was estimated based on corkscrew extraction experiments. This method involves initially rotating a corkscrew manually to the required depth (see supplementary material S2 and S3). A pulley equipped with a load cell, fixed to a tripod, is then used to extract the corkscrew from the soil while measuring the force. This test method proved advantageous as it allows for relatively quick and in-situ measurements of soil strength. The corkscrew extraction test was chosen due to its applicability in difficult terrain and its relatively non-destructive nature, which was necessary given the close proximity of the test site to the water body. Furthermore, it provided partially disturbed soil sample with roots, which were suitable for additional analyses such as determining Root Area Ratio (RAR) and Root Length Density (RLD). For a comprehensive description of the corkscrew test methodology and its specific application, please refer to the work of Meijer et al. (2018). The tests were conducted in June 2024.

The above-ground biomass was carefully removed using a sharp knife prior to testing. Due to a high-water table in the flat region immediately behind the sheet pile, tests were conducted up to a depth of 0.25 m. Generally, the observed rooting depth in the study area was limited to approximately 0.35 m. Therefore, tests were conducted at two depth ranges: 0–0.125 m and 0.125–0.25 m. Two sets of tests were performed at distinct distances from the canal to account for a visually apparent difference in above-ground shoot density and to assess any potential strength variation with increasing distance from the water source. The first set of tests was conducted Near the Canal (NC), approximately 1 m away. The second set was performed Away from the Canal (AC), at a distance of about 2 m from the canal.

Strength of the sample measured from corkscrew extraction (τ, kPa) was determined as:

$$\tau = \frac{F}{2\pi rh} \tag{1}$$

where F is the measured extraction force in kN, r is the radius of the corkscrew in m, and h is the height of the corkscrew in m. The increase in shear strength provided by roots ($\Delta\tau$) was determined as the difference between the strength of the rooted sample and the corresponding average bare soil strength.

2.3. Root traits and root strength measurement

Soil samples obtained from corkscrew samples were frozen to −20 °C to prevent decomposition. The soil plugs were taken out and were washed on a sieve (4 mm to 0.5 mm openings) to collect root material for scanning. The roots were then scanned using EPSON V850 Pro scanner. Further, RhizoVision Explorer (Seethepalli et al., 2021; Seethepalli and York, 2020) was used for image analysis. Segmented images were analysed to determine root length in different diameter classes and root volume. RLD was estimated as root length per soil volume. Assuming uniform distribution of root orientations, RAR was determined from root volume fraction (RV) following Bengough et al. (1992) and Meijer et al. (2018) as

$$RAR\left[m^2m^{-2}\right] = \frac{RV}{2}\left[m^3m^{-3}\right] \tag{2}$$

To further determine the root traits, a total of twelve soil blocks were excavated: six at the NC location and six at the AC location. Each excavation block measured 0.5 m × 0.5 m × 0.35 m. Following the procedure of Moulisova et al. (2023), three rhizome pieces, each containing a single node, were randomly selected in each excavation block. The characterization of root traits was conducted on three rhizome pieces from each excavation block to ensure a representative sample of root distribution within the large block size, while maintaining feasibility for laboratory processing. In total, 36 nodes were selected for analysis (12 blocks × 3 nodes/block). The number of adventitious roots growing from each node was counted. The adventitious roots were then cut from the rhizome, washed, and scanned as mentioned above.

The total number of root tips and number of root branches were measured. Length, surface area of the roots and RAR were estimated for 5 different diameter classes (0–0.5 mm, 0.5-1 mm, 1–1.5 mm, 1.5-2 mm, >2 mm). No distinction between lateral roots and adventitious roots were made. The root samples were then dried at 80^0C to constant weight and recorded as ́dry weight ́. Specific root length and specific surface area was estimated as ratio of root length to dry weight and root surface area to dry weight respectively. Further, total root length and surface area per square meter of canal bank was estimated using the total dry biomass of roots from each excavation. Total roots and rhizome from each excavation were dried at 80^0C to constant weight and recorded as corresponding dry weight.

Root tensile strength was measured on root samples obtained from the excavated root samples. The root samples were clamped using jaw clamps and tensile tested in a Universal Testing Machine. The roots were attached to small pieces of sandpaper to prevent slippage. The peak load and diameter of the root were recorded.

The contribution of roots to the soil shear strength is estimated using Wu & Waldron model (WWM) as (Waldron, 1977; Wu et al., 1979), Eq. (3):

$$C_r = k' \sum_i T_{r,i} RAR_i \quad (3)$$

where C_r is the cohesion due to roots in kPa, k' is a factor taking into account the root orientation, T_{ri} is the tension strength of the average root diameter in the diameter class in kPa and RAR is the root area ratio. The increase in shear strength provided by roots (Δτ) was determined as the difference between the strength of the rooted samples and the corresponding average bare soil strength.

2.4. Data analysis

Normality of data for the measured parameters was checked using the Shapiro-Wilk normality test. Measured corkscrew strength and RLD were found to be non-normally distributed ($p < 0.05$). Therefore, the non-parametric Mann-Whitney *U* test was used to compare differences between the NC and AC locations for these two parameters. The RAR data was found to be normally distributed. Levene's test was first conducted to check for homogeneity of variances. An Independent samples *t*-test was subsequently used to compare significant differences in the RAR between the NC and AC locations.

3. Results and discussion

3.1. Soil strength measurements

The bare soil within the tested area (NC and AC) had a baseline mean strength of 10.7 kPa (SD = 1.8, n = 5) at depth 0.125 m and 13.2 kPa (SD = 0.4, n = 5) at depth 0.25 m (Fig. 3). Tensiometers installed at an adjacent site at about 10 m from the test site showed zero suction during the testing period. The maximum strength for bare soil of 14.0 kPa was found at depth 0.25 m.

Tests at AC, had an average increase in strength of 6.6 kPa (SD = 1.8, n = 8) at depth 0.125 m and 7.4 kPa (SD = 3, n = 11) at depth 0.25 m (Fig. 4). While a maximum increase of 10.9 kPa was obtained, one data point at depth 0.25 m, had a decrease in strength of −1 kPa when compared to average strength of bare soil at depth 0.25 m. The observed increase in soil-root composite shear strength with *P.australis* roots aligns with studies demonstrating root reinforcement through mechanical binding and enhanced soil cohesion (De Baets et al., 2008; Yu et al., 2020; Li et al., 2024). However, the localized strength reduction highlights the system's complexity, consistent with findings that root reinforcement effects vary with depth and possible root degradation processes (De Baets et al., 2008; Phan et al., 2025). The observed variations could also be due to natural variability in local soil properties such as density, which can influence the soil component in the root-soil shear strength (Meijer et al., 2019).

Significant increase in average strength, 19.9 kPa (SD = 9.7, n = 8) and 16.3 kPa (SD = 9.4, n = 12) at depth 0.125 m and 0.25 m respectively was observed for NC. The maximum observed increase of 36.6 kPa at 0.25 m depth in NC underscores the reinforcing potential of *P.australis* roots in canal-adjacent soils. The increase in strength due to *P.australis* roots found for NC location is within the range of root reinforcement reported in literature. The C_r of vegetated soils exhibits considerable variation across species and environments and can typically fall in the order of tens of kPa (e.g., De Baets et al., 2008; Schwarz et al., 2010a; Török and Parker, 2022). However, most studies report C_r values within the narrower range of 1.0–30.0 kPa for typical herbaceous and shrub species (Burroughs and Thomas, 1977; Schmidt et al., 2001; Török and Parker, 2022). The higher extreme values (>50 kPa) are generally associated with mature woody vegetation or particularly dense root systems in optimal growing conditions.

The strength increases between NC and AC were significantly different ($p < 0.05$), suggesting that proximity to the canal may influence root development and soil-root interaction dynamics. This difference is further supported by root morphological parameters. The RAR was significantly higher in NC (mean 0.32 %) than in AC (mean 0.21 %), with a maximum of 0.65 % observed at NC and a minimum of 0.03 % at AC (Fig. 5). Li et al. (2024) suggested that in the range of 0–0.36 % an optimal RAR of 0.14 % maximized the contribution of roots to the shear

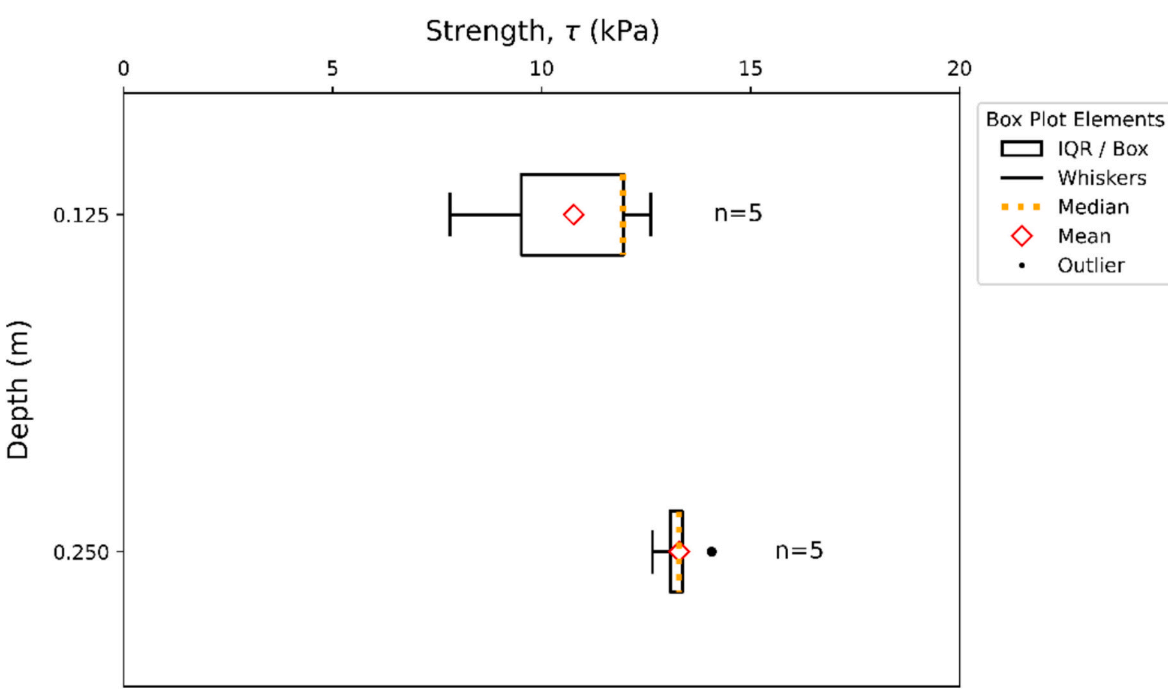

Fig. 3. Boxplot showing variation of bare soil strength (kPa) for two depth, 0.125 m and 0.250 m.

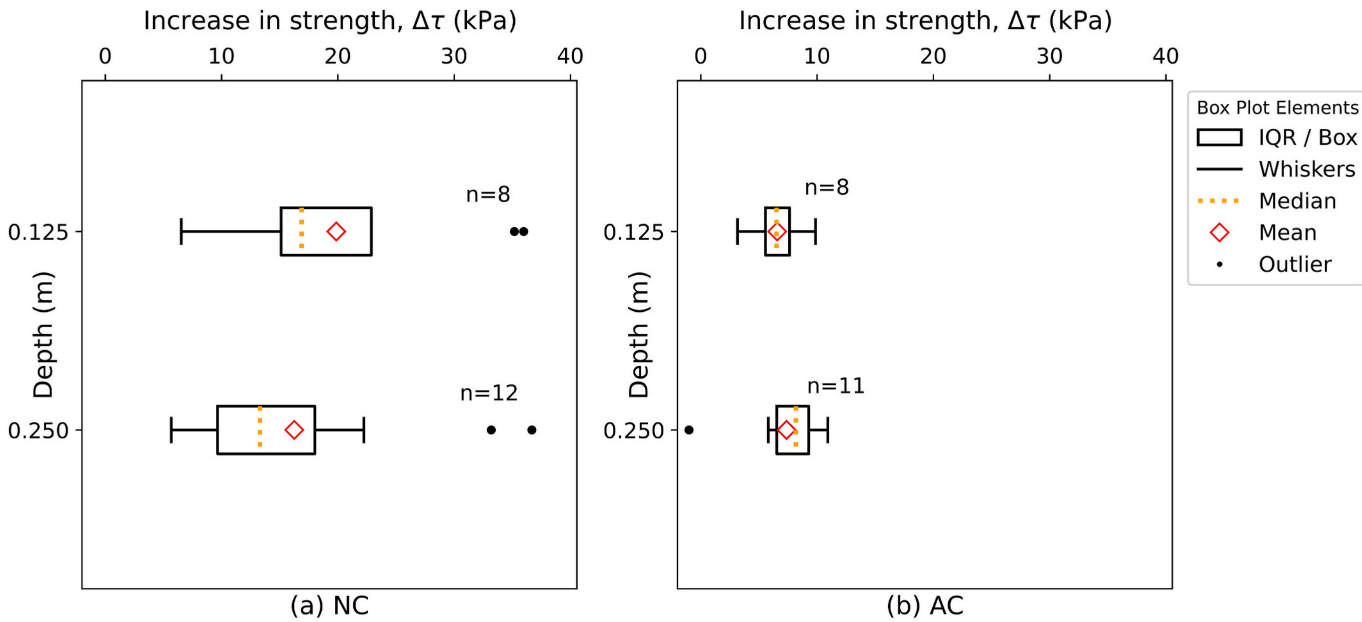

Fig. 4. Boxplots showing change in strength compared to average bare soil strength as measured at locations NC (a) and AC (b) at two depths 0.125 m and 0.250 m.

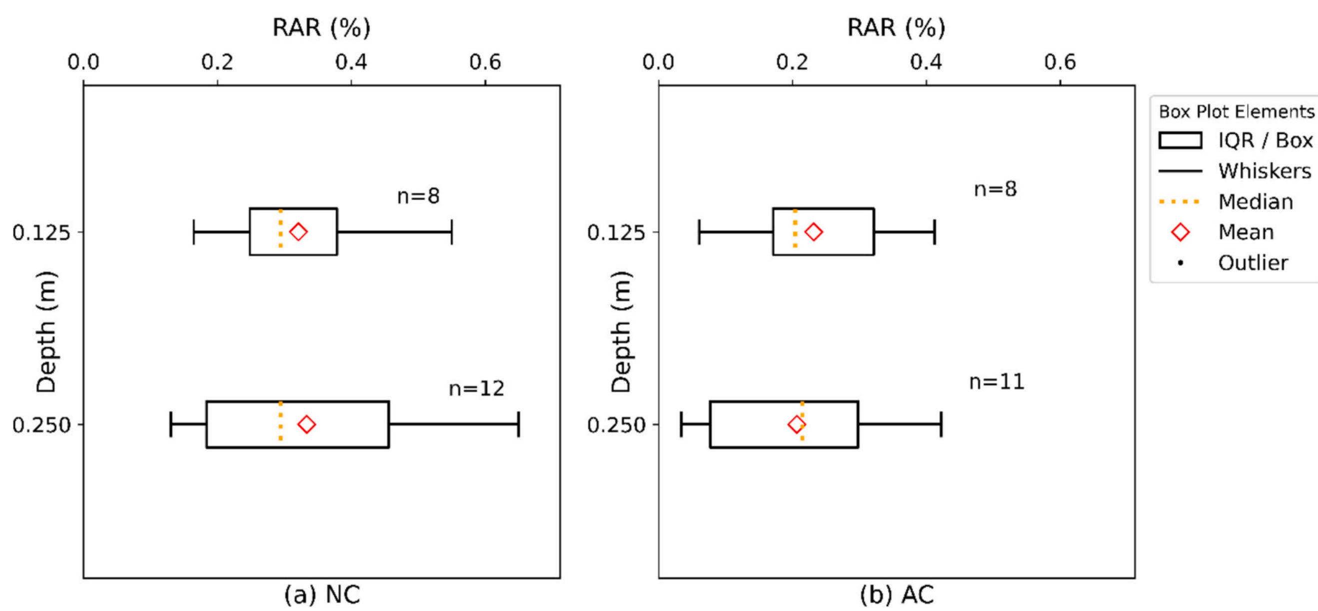

Fig. 5. Boxplots showing variation in root area ratio as measured at locations NC (a) and AC (b).

strength and cohesion. The RAR determined in this study was lower than RAR (0.35–0.95 %) for *P.australis* was reported by Yu et al. (2020) and within the range reported by De Baets et al. (2008).

The RAR data was found to be normally distributed and significant difference between NC and AC was found ($p < 0.05$). The RLD was also significantly higher for NC than AC tests ($p < 0.05$). The average total RLD of NC was 4.83 ± 2.10 cm/cm^3 and for AC was 2.58 ± 2.15 cm/cm^3 (Fig. 6). Roots in both NC and AC had an exponential decrease in RLD with an increase in root diameter class, with most of the root length being in the <0.5 mm diameter class. This could be due to a higher percentage of lateral roots in the total root length. The diameters of lateral roots are typically less than 0.5 mm (Li et al., 2021). Higher percentages of root lengths in thinner root classes relative to total length of root system were also observed by Moulisova et al. (2023).

3.2. Estimated increase in soil strength

The power law relationship between root diameter and measured tensile strength ($T_r = 9.41D^{-1.14}$, $R^2 = 0.67$) aligns with well-established biomechanical principles for plant roots (Fig. 7). The negative exponent and the coefficient of determination match the typical range reported for various species in global compilations (e.g., De Baets et al., 2008; Comino et al., 2010; Rossi et al., 2022). Specifically for *P.australis*, the measured tensile strength results of De Baets et al. (2008) are stronger than determined in this study. The root tensile strength depends among others on soil moisture content, root type, chemical composition, root age, decomposition (Genet et al., 2005; Loades et al., 2013; Boldrin et al., 2018).

C_r due to roots was estimated using the RAR and measured tensile strength via Eq. (3), assuming a conservative value of k' = 1. While k' typically ranges from 1.0 to 1.3 when roots intersect the shear plane

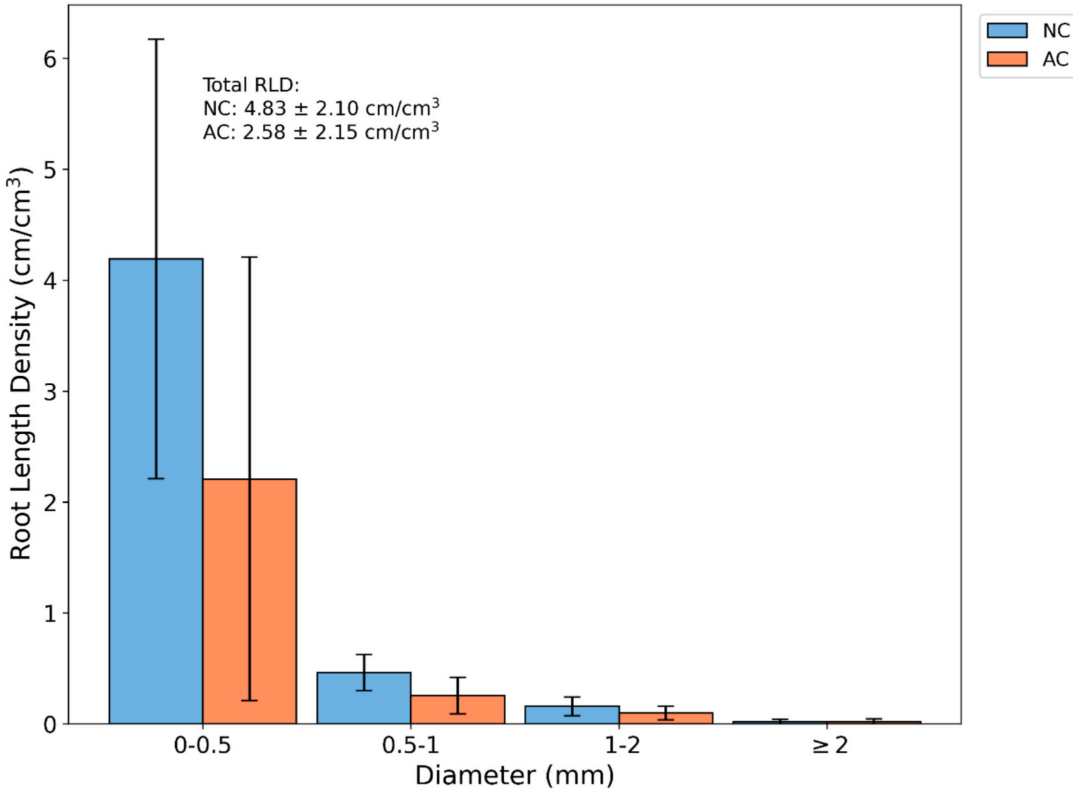

Fig. 6. RLD distribution across different root diameter classes for 'NC' and 'AC' locations. Bars represent the mean RLD for each diameter class, and error bars indicate the standard deviation. The total RLD along with standard deviation is given.

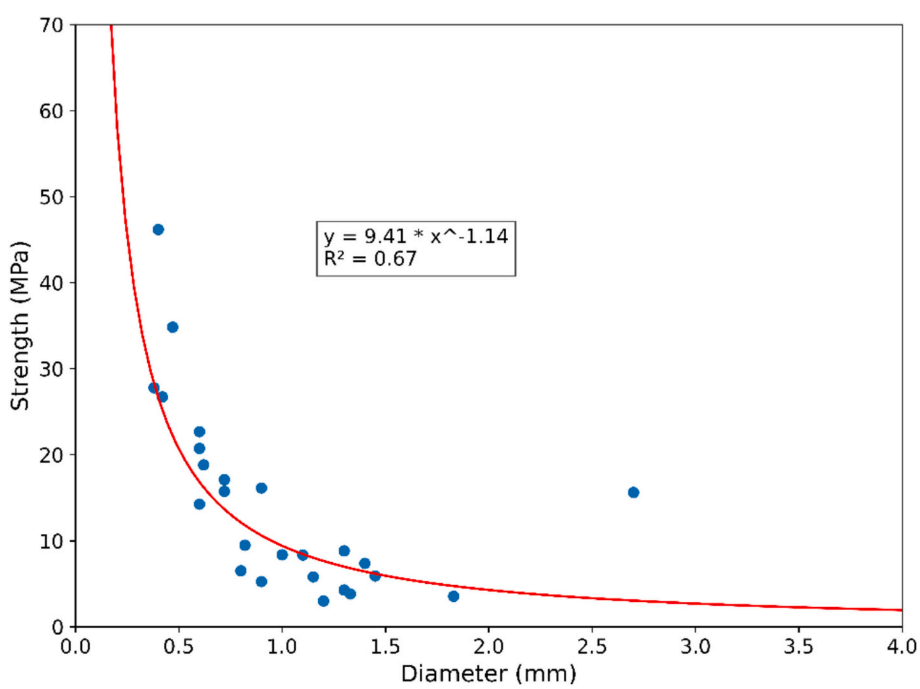

Fig. 7. Variation of measured tensile strength (MPa) of the *P.australis* roots with Diameter (mm).

perpendicularly—leading to common simplifications such as 1.15 (Waldron, 1977) or 1.2 (Wu et al., 1979)—Bischetti et al. (2010) emphasized its significant influence on cohesion estimates. However, Comino et al. (2010) supported using k' = 1 as a practical baseline for non-woody species such as *P.australis*, especially in the absence of site-specific calibration.

Fig. 8 shows the relationship between measured shear strength increase from corkscrew tests and estimated root cohesion via Eq. (3). The best-fit line has a slope of 0.26, indicating that the WWM overestimates in-situ reinforcement by approximately a factor of 3.8 (1/0.26). This aligns with Operstein and Frydman (2000), who reported a 400 % overestimation (slope ≈ 0.25), attributed to WWM's assumption of

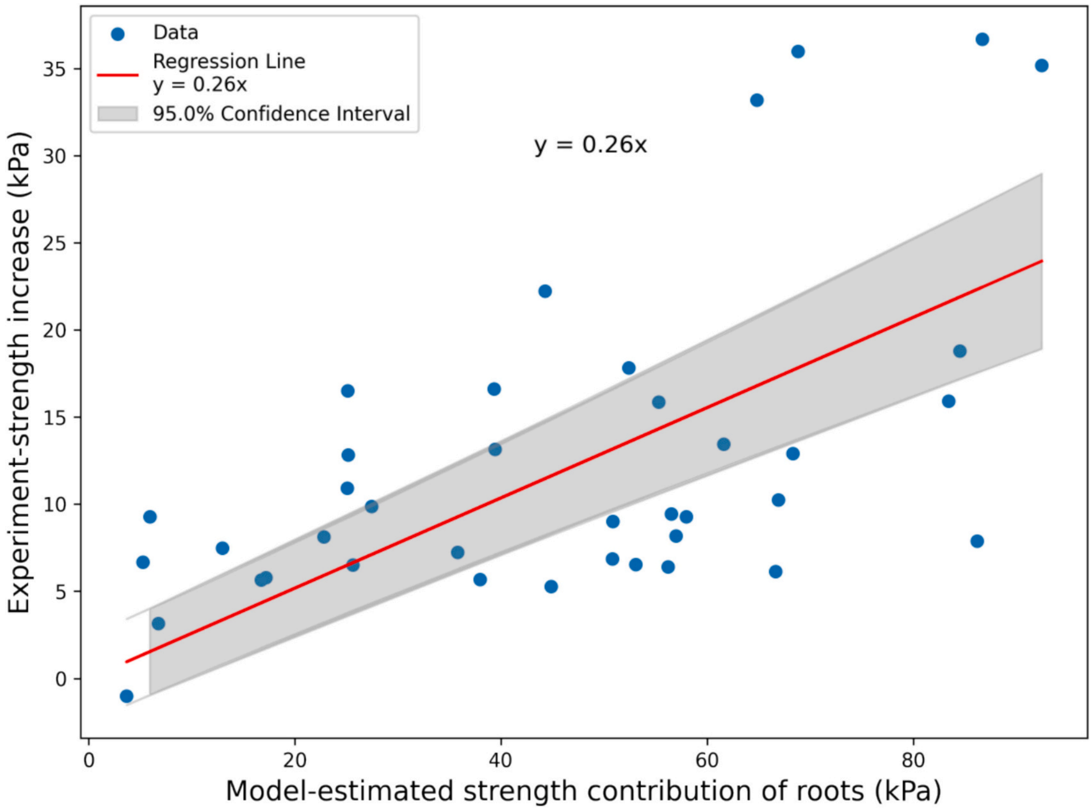

Fig. 8. Relationship between the model-estimated increase in strength due to roots and the increase of strength obtained from corkscrew experiments. The regression line (y = 0.26x) quantifies the observed systematic relationship.

simultaneous root breakage. Meijer et al. (2018) also found that corkscrew-derived k' values from surface layers were on the lower end of literature values, with lab-based k' values (under saturated conditions) consistently lower than field-based ones (at natural moisture content).

Fiber Bundle Models (FBMs) are an advanced alternative to WWM, simulating load sharing and progressive root failure (Pollen and Simon, 2005; Bischetti et al., 2010). A factor k″ can be used to link FBM outputs to WWM estimates (Comino et al., 2010). However, FBMs may over-predict cohesion by neglecting root slippage, particularly in case of herbaceous species like *P.australis* (Comino et al., 2010; Ji et al., 2020; Meijer, 2021). Although highly advanced models (e.g., Schwarz et al., 2010b) incorporate slippage, they demand a larger set of input parameters, which were not determined in this study (e.g., interfacial friction, root tortuosity).

Identifying the optimal model for *P.australis* is beyond this study's scope. Nonetheless, our corkscrew-derived reinforcement values (6–19 kPa) align with the lower bounds reported by Li et al. (2024) (9.97–18.69 kPa) and Yu et al. (2020) (mean 31.16 kPa), supporting the method's utility for tracking reinforcement evolution while avoiding overestimation biases.

Finally, our empirical slope of 0.26 falls within the reduction factor range (0.21–0.82) proposed by De Baets et al. (2008), reinforcing the value of corkscrew testing as a practical middle ground between simplistic models like WWM and parameter-intensive alternatives such as RipRoot.

3.3. Root structural traits

Average number of shoots at NC and AC were 117 (SD = 20) and 40 (SD = 10) respectively. Root structural traits determined for both locations and are summarized in Table 1. The mean number of adventitious roots growing from one node was 3 for both NC (range 3–6) and AC (range 1–5). The mean number of tips per meter root length was also comparable, at 208 m^{-1} (NC) and 210 m^{-1}(AC).

Table 1
Root structural traits in the NC and AC locations along the canal bank. Based on them are values extrapolated to 1 m^2 area of the bank. The numbers represent mean (Maximum; Minimum). The statistics for each location (NC and AC) are based on a total sample size of n = 18 nodes, derived from 6 excavations (3 nodes per excavation).

Trait	NC	AC
Number of samples (nodes)	18	18
No. of adventitious roots growing from one node	3 (6;3)	3 (5;1)
Dry weight of roots growing from one node (mg)	86 (145;35)	66 (111;18)
No. of tips per 1 m root length (m^{-1})	208 (362;150)	210 (307;150)
Branches frequency (mm^{-1})	1.53 (2.1;0.16)	1.1 (1,7;0.1)
Specific length of roots (m g^{-1})	77.8 (108.9;43.5)	60.6 (92.8;31.4)
Specific surface area of roots (m^2 g^{-1})	0.05 (0.07;0.03)	0.05 (0.09;0.02)
Values extrapolated to 1 m^2		
Length of roots (km m^{-2})	10.2	4.5
Surface area of roots (m^2 m^{-2})	7.8	3.9

Higher dry weight of roots was recorded for samples from NC, namely 86 mg, compared to 66 mg for samples from AC. The extrapolated values for 1 m^2 show that the total root length (10.2 km m^{-2}) and total surface area (7.8 m^2 m^{-2}) at NC were significantly higher than the corresponding values for AC (4.5 km m^{-2} and 3.9 m2 m^{-2}) respectively. Nevertheless, in both samples, the proportion of thinner roots (<0.5 mm) was significantly higher than other root diameter classes. The total root biomass was also higher for location NC than AC. Care should be taken in interpreting this data as no differentiation between adventitious roots and lateral roots could be made.

Average, total rhizome biomass at location NC was 415 g m^{-2} and at location AC was 211 g m^{-2} (Fig. 9). These values are generally in the lower range of the reported rhizome production rates for both constructed and natural wetlands. An average annual rhizome production of about 500–700 g m^{-2} in constructed wetlands was reported by Moulisova et al. (2023) and values between 400 and 600 g m^{-2} were reported by Čížková and Lukavská (1999) in natural wetlands. In natural stands, rhizomes have been reported to have life spans between four to six years (Čížková and Lukavská, 1999). Our study was conducted approximately 22 months after planting and the rhizome dry weight biomass found in this study is in general on the lower side of values reported in literature.

Consistent with findings by Li et al. (2014), the specific root length in this study falls within the ranges reported for aquatic reed (94.9 ± 29.2 m g^{-1}) and terrestrial reed (40.4 ± 18.1 m g^{-1}). The estimates of specific root length must be interpreted with caution and may be site-specific, largely due to the considerable variance observed in background data such as growth conditions and soil (Moulisova et al., 2023). This wide range is evident in other studies; for instance, Chen et al. (2017) reported values between 7 and 20 m g^{-1}, while Moulisova et al. (2023) documented ranges from 61 to 85 m g^{-1}.

3.4. Practical implications

While our results clearly demonstrate that *P.australis* provides substantial root reinforcement (average 6–19 kPa), making it a highly effective biotechnical tool for bank stabilization. This functional benefit, however, must be integrated with the ecological context discussed in the introduction. Therefore, its utilization must be integrated into a careful ecological management strategy. For our specific study area in the Netherlands, *P.australis* is a native species, yet its robust clonal expansion and capacity to form dense, monodominant stands may present an ecological challenge by potentially reducing native plant diversity and disrupting natural succession pathways. Therefore, management decisions must weigh the proven mechanical benefits, particularly in managed, high-value infrastructure like canals or engineered wetlands, against the necessity of maintaining local biodiversity. Our findings suggest that where aggressive colonization is already accepted or necessary (e.g., flood defence or highly disturbed, low-diversity areas), *P.australis* is mechanically beneficial. In ecologically sensitive or high-diversity areas, the mechanical gains must be critically compared against the risks of habitat alteration, potentially favouring less aggressive native species (e.g., Fogliata et al., 2021; Vila et al., 2011). Our data on the root reinforcement capacity of *P.australis* provides a critical quantitative metric that can help managers weigh these geotechnical and ecological factors when making decisions on bioengineered bank protections.

While this study focuses on the direct mechanical quantification of root reinforcement, the reported values for root area ratio and shear strength increase provide the necessary parameterization for bank-stability models such as Bank-Stability and Toe-Erosion Model (BSTEM). Future research could utilize these in-situ metrics to simulate long-term bank evolution and geomorphological stability in bioengineered systems.

4. Conclusions

This study provides comprehensive quantitative evidence of *Phragmites australis* L. effectiveness in soil reinforcement during establishment phase, through the direct measurement of root reinforcement using the corkscrew extraction technique. Spatial patterns were observed in root reinforcement between Near-Canal (NC) and Away-from-Canal (AC) locations, therefore providing a robust range of field reinforcement values for bioengineering design. The findings demonstrate that NC location exhibited substantially greater root reinforcement, with average shear strength increases of 19.9 kPa (SD = 9.7) at 0.125 m depth and 16.3 kPa (SD = 9.4) at 0.25 m, compared to modest improvements at AC location (6.6 kPa and 7.4 kPa at corresponding depths).

The primary reinforcement mechanism is driven by the dominance of fine roots (<0.5 mm diameter, constituting >80 % of root length), which create dense fibrous networks. Biomechanical testing revealed a power-law relationship between root diameter and tensile strength, consistent with global datasets. The average total root length estimated from total root biomass was 10.2 km m^{-2} and 4.5 km m^{-2} for NC and AC locations, respectively, explaining the observed difference in soil strength.

These results establish *P.australis* as a high-performance species for soil bioengineering techniques where high mechanical stabilization is required. The ability to directly quantify its reinforcement using the corkscrew method offers a robust path for calculating site-specific design parameters for the stabilization of streambanks and canal slopes.

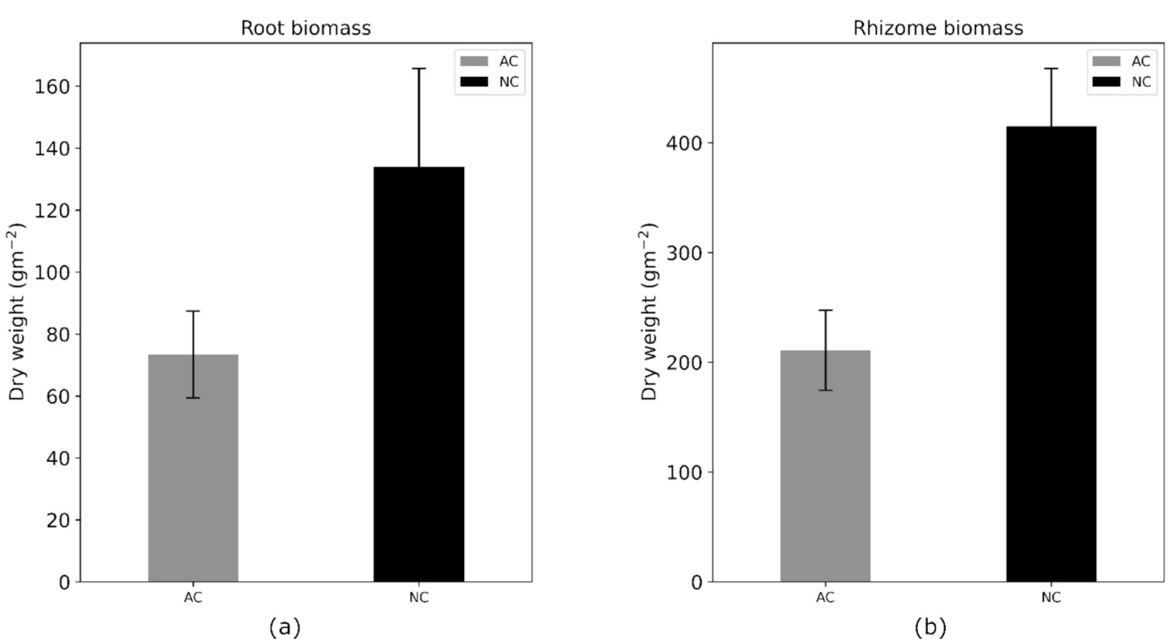

Fig. 9. Bar chart of dry weight of excavated root biomass (a) and rhizome (b) measured at AC and NC location from excavations.

CRediT authorship contribution statement

Abhijith Kamath: Writing – original draft, Visualization, Methodology, Investigation, Data curation. **Jan-willem van de Kuilen:** Writing – review & editing, Supervision, Project administration, Funding acquisition, Conceptualization.

Declaration of competing interest

The authors declare the following financial interests/personal relationships which may be considered as potential competing interests: Abhijith Kamath reports financial support was provided by Provincie Noord-Holland. If there are other authors, they declare that they have no known competing financial interests or personal relationships that could have appeared to influence the work reported in this paper.

Acknowledgements

The authors gratefully acknowledge the Provincie Noord-Holland and Centrum Hout for having funded the research study.

Appendix A. Supplementary data

Supplementary data to this article can be found online at https://doi.org/10.1016/j.geomorph.2026.110159.

Data availability

The authors do not have permission to share data.

References

Abernethy, B., Rutherfurd, I.D., 2000. Does the weight of riparian trees destabilize riverbanks? Regul. Rivers 16 (6), 565–576.
Andreoli, A., Chiaradia, E.A., Cislaghi, A., Bischetti, G.B., Comiti, F., 2020. Roots reinforcement by riparian trees in restored rivers. Geomorphology 370, 107389.
Bengough, A.G., Mackenzie, C.J., Diggle, A.J., 1992. Relations between root length densities and root intersections with horizontal and vertical planes using root growth modelling in 3-dimensions. Plant Soil 145 (2), 245–252.
Bischetti, G.B., Chiaradia, E.A., D'Agostino, V., Simonato, T., 2010. Quantifying the effect of brush layering on slope stability. Ecol. Eng. 36 (3), 258–264.
Boldrin, D., Leung, A.K., Bengough, A.G., 2018. Effects of root dehydration on biomechanical properties of woody roots of Ulex europaeus. Plant Soil 431, 347–369.
Boldrin, D., Bengough, A.G., Lin, Z., Loades, K.W., 2021. Root age influences failure location in grass species during mechanical testing. Plant Soil 461, 457–469.
Burroughs, R.J., Thomas, B.R., 1977. Declining root strength in Douglas-fir after felling as a factor in slope stability. In: U.S. Forest Service INT-190.
Capobianco, V., Robinson, K., Kalsnes, B., Ekeheien, C., Høydal, Ø., 2021. Hydro-mechanical effects of several riparian vegetation combinations on the streambank stability—a benchmark case in southeastern Norway. Sustainability 13 (7), 4046.
Carricondo, J.M., Oliver-Villanueva, J.V., Turégano, J.V., González, J.A., Mengual, J., 2021. Use of Phragmites australis for controlling phosphorus contamination in anthropogenic wetland ecosystems. Environ. Technol. 42 (19), 3055–3064.
Chen, Q., Wang, Y., Zou, C.B., Wang, Z.L., 2017. Aboveground biomass invariance masks significant belowground productivity changes in response to salinization and nitrogen loading in reed marshes. Wetlands 37, 985–995.
Čížková, H., Lukavská, J., 1999. Rhizome age structure of three populations of Phragmites australis (Cav.) Trin. ex Steud.: biomass and mineral nutrient concentrations. Folia Geobot. 34, 209–220.
Comino, E., Marengo, P., Rolli, V., 2010. Root reinforcement effect of different grass species: a comparison between experimental and models results. Soil Tillage Res. 110 (1), 60–68.
De Baets, S., Poesen, J., Reubens, B., Wemans, K., De Baerdemaeker, J., Muys, B., 2008. Root tensile strength and root distribution of typical Mediterranean plant species and their contribution to soil shear strength. Plant Soil 305, 207–226.
Ferrario, C., Peruzzi, C., Cislaghi, A., Polesello, S., Valsecchi, S., Lava, R., Zanon, F., Santovito, G., Barausse, A., Bonato, M., 2022. Assessment of reed grasses (phragmites australis) performance in PFAS removal from water: a phytoremediation pilot plant study. Water 14 (6), 946.
Fogliata, P., Cislaghi, A., Sala, P., Giupponi, L., 2021. An ecological analysis of the riparian vegetation for improving the riverine ecosystem management: the case of Lombardy region (North Italy). Landsc. Ecol. Eng. 17 (3), 375–386.
Genet, M., Stokes, A., Salin, F., Mickovski, S.B., Fourcaud, T., Dumail, J.F., Van Beek, R., 2005. The influence of cellulose content on tensile strength in tree roots. Plant Soil 278, 1–9.
Geurts, J.J.M., Oehmke, C., Lambertini, C., Eller, F., Sorrell, B.K., Mandiola, S.R., Grootjans, A.P., Brix, H., Wichtmann, W., Lamers, L.P.M., Fritz, C., 2020. Nutrient removal potential and biomass production by Phragmites australis and *Typha latifolia* on European rewetted peat and mineral soils. Sci. Total Environ. 747, 141102. https://doi.org/10.1016/j.scitotenv.2020.141102.
Haslam, S.M., 1970. The performance of Phragmites communis Trin. in relation to water-supply. Ann. Bot. 34 (4), 867–877.
Haslam, S.M., 1972. *Phragmites communis* Trin. (biological flora of the British Isles). J. Ecol. 60 (2), 585–610.
Ji, J., Mao, Z., Qu, W., Zhang, Z., 2020. Energy-based fibre bundle model algorithms to predict soil reinforcement by roots. Plant Soil 446 (1), 307–329.
Krzeminska, D., Kerkhof, T., Skaalsveen, K., Stolte, J., 2019. Effect of riparian vegetation on stream bank stability in small agricultural catchments. Catena 172, 87–96.
Li, C., Ding, S., Ma, X., Chen, M., Zhong, Z., Zhang, Y., Ren, M., Zhang, M., Yang, L., Rong, N., Wang, Y., 2021. O_2 distribution and dynamics in the rhizosphere of Phragmites australis, and implications for nutrient removal in sediments. Environ. Pollut. 287, 117193. https://doi.org/10.1016/j.envpol.2021.117193.
Li, L., Han, W., Thevs, N., Jia, X., Ji, C., Jin, D., He, P., Schmitt, A.O., Cirella, G.T., Zerbe, S., 2014. A comparison of the functional traits of common reed (Phragmites australis) in Northern China: Aquatic vs. terrestrial ecotypes. PLoS ONE 9 (2), e89063.
Li, X., Jin, K., Qin, P., Liu, C., Zhu, X., Zhang, Y., Zong, Q., 2024. Enhancement effect of phragmites australis roots on soil shear strength in the Yellow River Delta. Sustainability 16 (23), 10657.
Loades, K.W., Bengough, A.G., Bransby, M.F., Hallett, P.D., 2013. Biomechanics of nodal, seminal and lateral roots of barley: effects of diameter, waterlogging and mechanical impedance. Plant Soil 370, 407–418.
Meijer, G., Bengough, G., Knappett, J., Loades, K., Nicoll, B., 2019. Measuring the strength of root-reinforced soil on steep natural slopes using the corkscrew extraction method. Forests 10 (12), 1135.
Meijer, G.J., 2016. New Methods for In Situ Measurement of Mechanical Root-reinforcement on Slopes. Doctoral dissertation. University of Dundee.
Meijer, G.J., 2021. A generic form of fibre bundle models for root reinforcement of soil. Plant Soil 468 (1), 45–65.
Meijer, G.J., 2024. Improving power law fitting of root tensile strength–diameter relationships. Plant Soil 1–26.
Meijer, G.J., Bengough, A.G., Knappett, J.A., Loades, K.W., Nicoll, B.C., 2018. In situ measurement of root reinforcement using corkscrew extraction method. Can. Geotech. J. 55 (10), 1372–1390.
Moulisova, L., Čížková, H., Dušek, J., Kazda, M., 2023. Root and rhizome traits of the common reed (Phragmites australis) in a constructed wetland for wastewater treatment. Ecol. Eng. 186, 106832.
Operstein, V., Frydman, S., 2000. The influence of vegetation on soil strength. Proc. Inst. Civ. Eng. Ground Improv. 4 (2), 81–89.
Pagter, M., Brix, H., Baattrup-Pedersen, A., 2005. Tolerance and physiological responses of *Phragmites australis* to water deficit. Aquat. Bot. 81 (4), 285–299.
Phan, T.N., Leung, A.K., Nguyen, T.S., Kamchoom, V., Likitlersuang, S., 2025. Modelling root decomposition effects on root reinforcement and slope stability. Comput. Geotech. 179, 107024.
Pollen, N., Simon, A., 2005. Estimating the mechanical effects of riparian vegetation on stream bank stability using a fiber bundle model. Water Resour. Res. 41 (7).
Rey, F., Bifulco, C., Bischetti, G.B., Bourrier, F., De Cesare, G., Florineth, F., Graf, F., Marden, M., Mickovski, S.B., Phillips, C., Peklo, K., Poesen, J., Polster, D., Preti, F., Rauch, H.P., Raymond, P., Sangalli, P., Tardio, G., Stokes, A., 2019. Soil and water bioengineering: practice and research needs for reconciling natural hazard control and ecological restoration. Sci. Total Environ. 648, 1210–1218.
Romero, J.A., Brix, H., A. F., Comín, 1999. Interactive effects of N and P on growth, nutrient allocation and NH4 uptake kinetics by Phragmites australis. Aquat. Bot. 64 (3–4), 369–380.
Rossi, R., Picuno, P., Fagnano, M., Amato, M., 2022. Soil reinforcement potential of cultivated cardoon (Cynara cardunculus L.): first data of root tensile strength and density. Catena 211, 106016.
Rudrappa, T., Choi, Y.S., Levia, D.F., Legates, D.R., Lee, K.H., Bais, H.P., 2009. Phragmites australis root secreted phytotoxin undergoes photo-degradation to execute severe phytotoxicity. Plant Signal. Behav. 4 (6), 506–513.
Schmidt, K.M., Roering, J.J., Stock, J.D., Dietrich, W.E., Montgomery, D.R., Schaub, A.T., 2001. The variability of root cohesion as an influence on shallow landslide susceptibility in the Oregon Coast Range. Can. Geotech. J. 38 (5), 995–1024.
Schwarz, M., Cohen, D., Or, D., 2010a. Root-soil mechanical interactions during pullout and failure of root bundles. J. Geophys. Res.: Earth Surf. 115 (F4).
Schwarz, M., Lehmann, P., Or, D., 2010b. Quantifying lateral root reinforcement in steep slopes–from a bundle of roots to tree stands. Earth Surf. Process. Landf. 35 (3), 354–367.
Seethepalli, A., York, L.M., 2020. RhizoVision Explorer-interactive software for generalized root image analysis designed for everyone (Version 2.0. 2). In: Zenodo.
Seethepalli, A., Dhakal, K., Griffiths, M., Guo, H., Freschet, G.T., York, L.M., 2021. RhizoVision Explorer: open-source software for root image analysis and measurement standardization. AoB Plants 13 (6), plab056.
Simon, A., Collison, A.J., 2002. Quantifying the mechanical and hydrologic effects of riparian vegetation on streambank stability. Earth Surf. Process. Landf. 27 (5), 527–546.
Török, G.T., Parker, G., 2022. The influence of riparian woody vegetation on bankfull alluvial river morphodynamics. Sci. Rep. 12 (1), 18141.
Uchida, T., Tazaki, F., 2005. New methods and allelopathic considerations of riparian buffer zones using Phragmites australis (Cav.) Trin. Ecol. Eng. 24 (5), 559–569.

Uddin, M.N., Robinson, R.W., 2018. Can nutrient enrichment influence the invasion of Phragmites australis? Sci. Total Environ. 613, 1449–1459.
Vila, M., Espinar, J.L., Hejda, M., Hulme, P.E., 2011. Ecological impacts of invasive alien plants: a meta-analysis of their effects on species, communities and ecosystems. Ecol. Lett. 14, 702–708.
Waldron, L.J., 1977. The shear resistance of root-permeated homogeneous and stratified soil. Soil Sci. Soc. Am. J. 41 (5), 843–849.
Wang, X., Yu, J., Zhou, D., Dong, H., Li, Y., Lin, Q., Guan, B., Wang, Y., 2012. Vegetative ecological characteristics of restored reed (Phragmites australis) wetlands in the Yellow River Delta, China. Environ. Manage. 49 (2), 325–333.
Wu, T.H., McKinnell III, W.P., Swanston, D.N., 1979. Strength of tree roots and landslides on Prince of Wales Island, Alaska. Can. Geotech. J. 16 (1), 19–33.
Yu, G.A., Li, Z., Yang, H., Lu, J., Huang, H.Q., Yi, Y., 2020. Effects of riparian plant roots on the unconsolidated bank stability of meandering channels in the Tarim River, China. Geomorphology 351, 106958.
Zhang, D., Cheng, J., Liu, Y., Zhang, H., Ma, L., Mei, X., Sun, Y., 2018. Spatio-temporal dynamic architecture of living brush mattress: root system and soil shear strength in riverbanks. Forests 9 (8), 493.